Bifurcations on the fcc lattice

T. K. Callahan and E. Knobloch
Department of Physics, University of California, Berkeley, California 94720
(Received 27 April 1995)

Pattern formation arising from the Turing instability in three dimensions is considered. Two three-dimensional patterns, with fcc and double-diamond structure, are found. These can be stable for realistic parameter values in the Brusselator model of the instability.

PACS number(s): 47.54.+r, 47.20.Ky, 02.20.−a

Recent experiments on the Turing instability [1] have stimulated renewed interest in the formation of spatially periodic patterns in three dimensions. In contrast to the much studied pattern-forming instabilities in hydrodynamics the length scale of the Turing instability is determined by local diffusion coefficients and thus is unrelated to any externally imposed length scale. Consequently such an instability readily produces three-dimensional patterns, provided only that its length scale is small relative to the dimensions of the apparatus. In this paper we show, quite generally, that instabilities of this kind can lead to two new types of stable three-dimensional (3D) patterns, one with fcc structure and the other with double-diamond structure, and illustrate the results using the Brusselator model of the Turing instability.

We assume the medium is isotropic and homogeneous, and the instability enters with wave number k_c. We look for spatially periodic patterns and hence pose the problem on a triply periodic lattice produced by wave vectors $\mathbf{k}$ with $|\mathbf{k}|=k_c$. This assumption allows us to formulate the problem as a finite-dimensional equivariant bifurcation problem [2]. It also limits our stability analysis to perturbations defined on the lattice, but related calculations on the bcc [3,4] and 2D hexagonal [5] lattices have been confirmed by experiments [6] and numerical simulations [4,5].

Although there is a large number of possible lattices in three dimensions [7] we focus here, in contrast to earlier work [3,4], on the face-centered-cubic (fcc) lattice. Our choice implies the selection of 8 marginally stable wave vectors from the sphere, corresponding to the vertices of a cube. We write these as $\pm\mathbf{k}_j$, where

$$\mathbf{k}_1=\frac{k_c}{\sqrt{3}}(1,1,1),\quad \mathbf{k}_2=\frac{k_c}{\sqrt{3}}(1,-1,-1),$$

$$\mathbf{k}_3=\frac{k_c}{\sqrt{3}}(-1,1,-1),\quad \mathbf{k}_4=\frac{k_c}{\sqrt{3}}(-1,-1,1) \tag{1}$$

relative to Cartesian coordinates (x,y,z). The symmetry of the problem is given by the symmetry of the unit cell (the cube) together with translations in the three principal directions. This group is $\Gamma=T^3\dot{+}\mathbb{O}\oplus\mathbb{Z}_2$, where T^3 is the three-torus of translations, $\mathbb{O}$ is the group of all orientation-preserving symmetries of the cube, and the nontrivial element of $\mathbb{Z}_2$ represents inversion through the origin.

Any scalar quantity X with the periodicity of the lattice can be written in the form

$$X(\mathbf{x},t)=\sum_{j=1}^{4}(z_j e^{i\mathbf{k}_j\cdot\mathbf{x}}+\bar{z}_j e^{-i\mathbf{k}_j\cdot\mathbf{x}})+(\text{higher-order terms}) \tag{2}$$

for some set of complex amplitudes $z_j(t)$. In order that the functions $X(\gamma\mathbf{x},t)$ obtained by applying the symmetries $\gamma\in\Gamma$ also be solutions, the evolution equations for the (complex) amplitudes $z_j(t)$ must be Γ equivariant; i.e., they must commute with an appropriate representation of Γ. The most general such equations can be written in the form [8]

$$\dot{z}_1=z_1(h_1+u_1h_3+u_1^2h_5+u_1^3h_7)+\bar{z}_2\bar{z}_3\bar{z}_4(p_3+u_1p_5+u_1^2p_7+u_1^3p_9), \tag{3}$$

where each h and p is an arbitrary real-valued function of the five elementary Γ invariants σ_1, σ_2, σ_3, σ_4, q and a distinguished bifurcation parameter λ. Here

$$\sigma_1=u_1+u_2+u_3+u_4, \tag{4a}$$

$$\sigma_2=u_1u_2+u_1u_3+u_1u_4+u_2u_3+u_2u_4+u_3u_4, \tag{4b}$$

$$\sigma_3=u_1u_2u_3+u_1u_2u_4+u_1u_3u_4+u_2u_3u_4, \tag{4c}$$

$$\sigma_4=u_1u_2u_3u_4, \tag{4d}$$

$$q=z_1z_2z_3z_4+\bar{z}_1\bar{z}_2\bar{z}_3\bar{z}_4, \tag{4e}$$

and $u_i=|z_i|^2$. The equations for $\dot{z}_2$, etc., follow from the requirement of Γ equivariance.

By rescaling $\mathbf{z}$, t, and λ we can transform Eqs. (3) into

$$\dot{z}_1=z_1(\lambda+a\sigma_1+u_1)+c\bar{z}_2\bar{z}_3\bar{z}_4+O(\mathbf{z}^5), \tag{5}$$

where

$$a=\frac{h_{1,\sigma_1}}{h_3},\quad c=\frac{p_3}{h_3}, \tag{6}$$

evaluated at $\lambda=\sigma_1=\sigma_2=\sigma_3=\sigma_4=q=0$. If $h_3<0$, the stable eigenvalues of (5) correspond to unstable eigenvalues of the original system (3), and *vice versa.* The truncated equations form a special case of those studied in Ref. [9].

The system (5) has the trivial solution $\mathbf{z}=0$ corresponding to the spatially uniform state of the system. In the following we assume the nondegeneracy conditions $a\neq-1,-1/2$; $4a\pm c\neq-1$; $c\neq0,\pm1$; $(3+c^2)a+1+c^2\neq0$. Near $\lambda=0$

TABLE I. The primary solution branches on the fcc lattice.

Branch	(z_1,z_2,z_3,z_4)	σ_1	Branching equation
0	(0,0,0,0)	0	$\sigma_1=0$
1	$(x,0,0,0)$	x^2	$h_{1,\lambda}\lambda+(h_{1,\sigma_1}+h_3)\sigma_1=O(4)$
2	$(x,x,0,0)$	$2x^2$	$h_{1,\lambda}\lambda+\frac{1}{2}(2h_{1,\sigma_1}+h_3)\sigma_1=O(4)$
3^+	(x,x,x,x)	$4x^2$	$h_{1,\lambda}\lambda+\frac{1}{4}(4h_{1,\sigma_1}+h_3+p_3)\sigma_1=O(4)$
3^-	$(-x,x,x,x)$	$4x^2$	$h_{1,\lambda}\lambda+\frac{1}{4}(4h_{1,\sigma_1}+h_3-p_3)\sigma_1=O(4)$
4	(y,x,x,x)	$y=(p_3/h_3)x$	$h_{1,\lambda}\lambda+(3h_{1,\sigma_1}+h_3)x^2+(h_{1,\sigma_1}+h_3)y^2=O(4)$

there are five branches of nontrivial equilibria, whose forms are given in Table I. The nondegeneracy conditions guarantee that these solutions, and no others, exist near $\lambda=0$. The existence of the first four of these solution branches is also guaranteed group theoretically by the equivariant branching lemma [2]. The solution branches can be found by restricting Eqs. (5) to the four solution types, and are given in Table I. The signs of the eigenvalues describing the stability properties of each of these patterns with respect to perturbations on the fcc lattice are listed in Table II. Note that solutions 2 and 4 can *never* be stable, while at most one of $3^\pm$ can be stable.

Branch 1 represents simple rolls or lamellæ, while the unstable solution 2 represents a rhombohedral prism state. Of greatest interest are the two potentially stable three-dimensional states $3^\pm$. The branch 3^+ represents a solution whose maxima and minima each form a face-centered cubic lattice. The remaining solution, 3^-, has the form

$$X(\mathbf{x})=-\cos(\mathbf{k}_1\cdot\mathbf{x})+\cos(\mathbf{k}_2\cdot\mathbf{x})+\cos(\mathbf{k}_3\cdot\mathbf{x})+\cos(\mathbf{k}_4\cdot\mathbf{x})+(\text{higher-order terms}), \tag{7}$$

having maxima and minima at $\frac{1}{8}L(2l+1,2m+1,2n+1)$. Here $L\equiv 2\pi/k_c$ and l, m, and n are integers satisfying

$$\begin{aligned} &l+m+n=0,1 \pmod 4 \text{ and all same parity (maxima)}\\ &l+m+n=2,3 \pmod 4 \text{ and all same parity (minima)}. \end{aligned} \tag{8}$$

The maxima thus form a diamond lattice, with two points at $\pm\frac{1}{8}L(1,1,1)$. The minima form another, interlocking, diamond lattice, shifted by $\frac{1}{2}L(1,1,1)$ from the maxima. By analogy with solid state physics [10] we refer to this as the double-diamond solution. The solutions $3^\pm$ are illustrated in Fig. 1. The remaining solution 4 has *submaximal* isotropy and can be thought of as a particular (nonlinear) superposition of $3^\pm$. In contrast to other problems of this type [9] this branch is *always* present.

As shown in Fig. 2 the nondegeneracy conditions divide the parameter space into 26 regions with different bifurcation diagrams. The regions containing stable solutions are listed in Table II. The six possible bifurcation diagrams containing stable solutions are shown in Fig. 3.

Thus far our analysis has been model independent, but for illustration we look at a concrete example, the Brusselator model of the Turing instability. This model is defined by

$$\dot{X}=D_x\nabla^2X-(B+1)X+X^2Y+A, \tag{9a}$$

$$\dot{Y}=D_y\nabla^2Y+BX-X^2Y, \tag{9b}$$

where A, B, X, and Y are chemical concentrations, A, B being kept in constant supply, and D_x, D_y are the diffusivi-

TABLE II. The eigenvalues of the solution branches on the fcc lattice, and the regions where stable branches exist. (Bold means stable for $h_3<0$, plain means stable for $h_3>0$.)

Branch	Eigenvalues	Regions of stability
0	λ(8 times)	All
1	$h_{1,\sigma_1}+h_3,-h_3$(6 times), 0(once)	A, B, C, D, E, F
2	$2h_{1,\sigma_1}+h_3,h_3,-(h_3\pm p_3)$(twice each), 0(twice)	∅
3^+	$4h_{1,\sigma_1}+h_3+p_3,-p_3,h_3-p_3$(3 times), 0(3 times)	B, G, **K**, **L**
3^-	$4h_{1,\sigma_1}+h_3-p_3,+p_3,h_3+p_3$(3 times), 0(3 times)	E, H, **I**, **J**
4	$(3h_{1,\sigma_1}+h_3)x^2+(h_{1,\sigma_1}+h_3)y^2$, $h_3(h_3^2-p_3^2)$(twice), $-h_3(h_3^2-p_3^2),-h_3$, 0(3 times)	∅

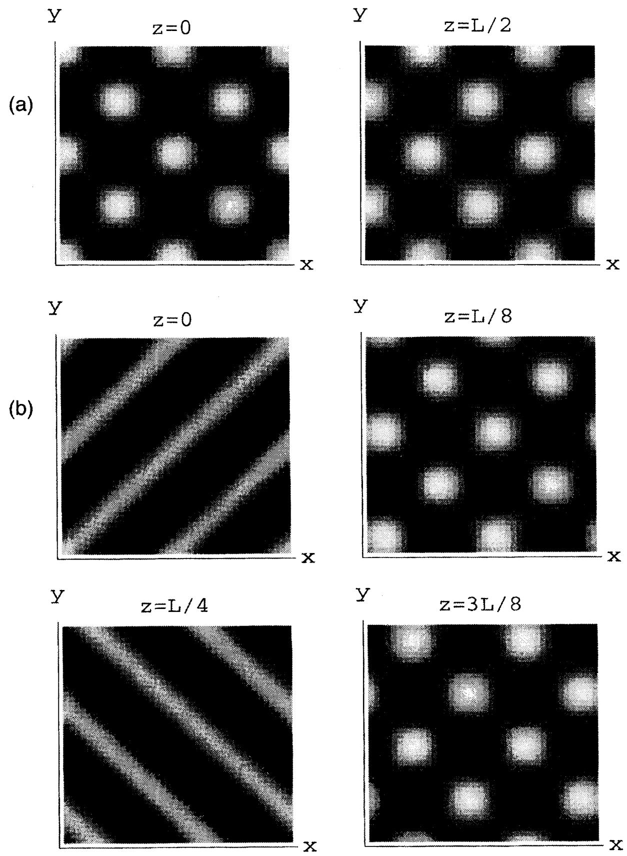

FIG. 1. The (a) fcc and (b) double-diamond solutions shown by means of horizontal sections. The grey scale indicates the magnitude of $X(\mathbf{x})$, with white denoting maximum and black minimum.

ties of X, Y, respectively. Traditionally, B is considered the bifurcation parameter. The equilibrium $(X,Y)\equiv(A,B/A)$ is then unstable with respect to perturbations of the form $e^{i\mathbf{k}\cdot\mathbf{x}}$, when $B>B(\mathbf{k})$. The curve $B(\mathbf{k})$ has a minimum at $|\mathbf{k}|^2=k_c^2\equiv A/\sqrt{D_xD_y}$ and $B(k_c)=B_c\equiv[1+A\sqrt{D_x/D_y}]^2$. Modes with this wave number are the first to lose stability as B increases.

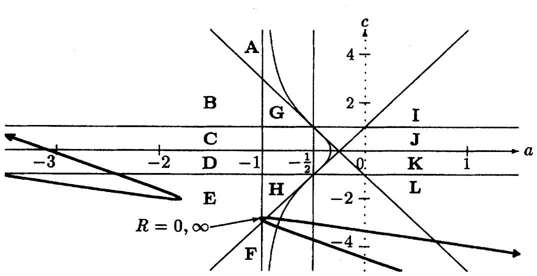

FIG. 2. The (a,c) plane showing the regions with different bifurcation diagrams. The solid line indicates the location of the Brusselator model as a function of R, with R increasing in the direction of the arrows. For the right branch $h_3<0$, while for the left branch $h_3>0$.

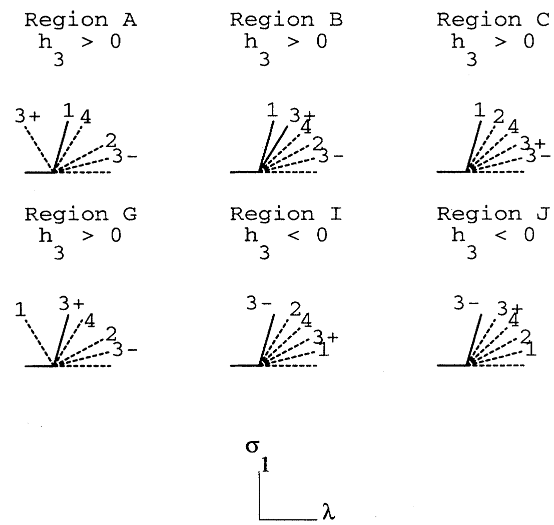

FIG. 3. The six bifurcation diagrams σ_1 vs λ (with $c>0$) containing stable solutions, labeled by region. The stable branches are denoted by a solid line. In regions B, I of Fig. 2 the relative amplitude of branches 1 and 3^+ depends upon c. We assume in these cases that $1<c<3$. For $c<0$ the diagrams are the same, but with the labels 3^+ and 3^- interchanged.

In order to make specific predictions for this model we have computed the coefficients h_{1,σ_1}, h_3, and p_3 using center manifold reduction, obtaining [11]

$$h_{1,\sigma_1}=\Delta\,\frac{1296-1036R-1706R^2+1296R^3}{75}, \tag{10a}$$

$$h_3=\Delta\,\frac{-11464+8374R+15229R^2-11464R^3}{675}, \tag{10b}$$

$$p_3=\Delta(48-36R-62R^2+48R^3). \tag{10c}$$

Here $R\equiv A\sqrt{D_x/D_y}=\sqrt{B_c}-1$ and Δ is an arbitrary, positive, irrelevant constant. As a result we predict that with respect to perturbations defined on the fcc lattice, rolls are stable for $0.894<R<1.297$, the fcc structure is stable for $0.855<R<0.907$ or $1.265<R<1.329$, and the double diamond structure is stable for $0.925<R<1.228$. This parameter region is outside that explored in recent simulations [4], which have concentrated on considerably higher values of R, suggesting that it might be fruitful to look for interesting structures at lower values of R. Note, however, that the possibility of a stable double-diamond structure is not specific to the Brusselator model. As shown here such patterns are expected to be present generically in models of three-dimensional instabilities.

This work was supported in part by the National Science Foundation under Grant No. DMS-9406144. We are indebted to A. De Wit for helpful discussions.

[1] V. Castets, E. Dulos, J. Boissonade, and P. De Kepper, Phys. Rev. Lett. **64**, 2953 (1990); Q. Ouyang and H. L. Swinney, Nature **352**, 610 (1991).
[2] M. Golubitsky, J. W. Swift, and E. Knobloch, Physica D **10**, 249 (1984); M. Golubitsky and D. Schaeffer, *Singularities and Groups in Bifurcation Theory* (Springer, Berlin, 1988), Vol. II.
[3] D. Walgraef, G. Dewel, and P. Borkmans, Adv. Chem. Phys. **49**, 311 (1982).
[4] A. De Wit, G. Dewel, P. Borckmans, and D. Walgraef, Physica D **61**, 289 (1992).
[5] A. De Wit, Ph.D. thesis, Université Libre de Bruxelles, 1993.
[6] J. J. Perraud, K. Agladze, E. Dulos, and P. De Kepper, Physica A **188**, 1 (1992).
[7] B. Dionne and M. Golubitsky, ZAMP **43**, 36 (1992); B. Dionne, *ibid.* **44**, 673 (1993).
[8] T. K. Callahan and E. Knobloch (unpublished).
[9] M. Silber and E. Knobloch, Nonlinearity **4**, 1069 (1991).
[10] C. Kittel, *Introduction to Solid State Physics*, 6th ed. (Wiley, New York, 1986).
[11] The quantity $h_{1,\sigma_1}+h_3$ has been calculated before. See A. De Wit (Ref. [5]), Appendix B.

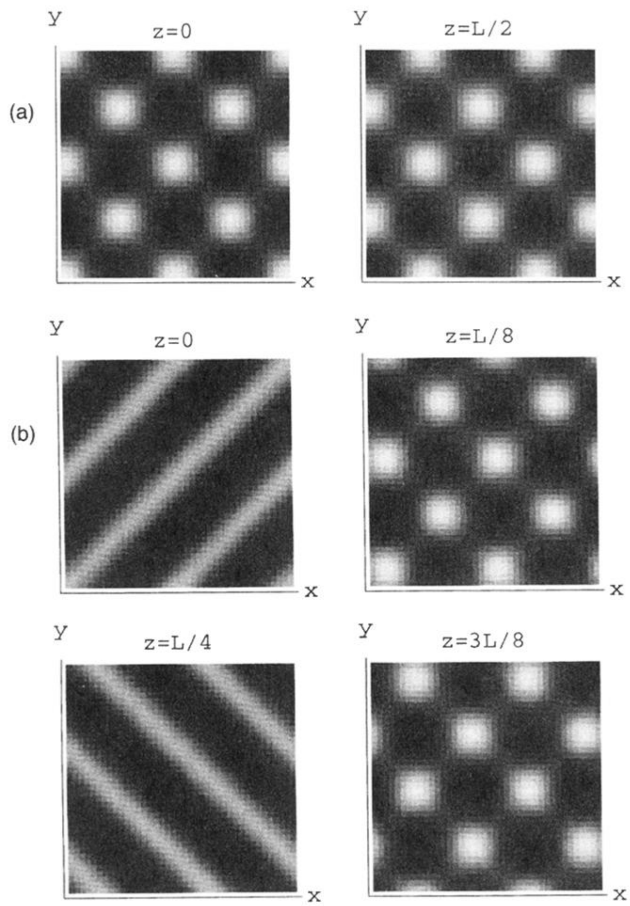

FIG. 1. The (a) fcc and (b) double-diamond solutions shown by means of horizontal sections. The grey scale indicates the magnitude of $X(\mathbf{x})$, with white denoting maximum and black minimum.